TABLE 2: Total mtDNA Sequencing Identified 16 Alterations Previously Reported as Polymorphisms, 10 Alterations in the MITOMAP Database, and 9 in the GiiB-JST mtSNP Database

Gene Product	Nucleotide Number	Base Change	Amino Acid Change	MITOMAP Database	GiiB-JST mtSNP Database
Hypervariable segment 2	200	A to G		Reported polymorphism	
Hypervariable segment 2	257	A to G		Reported polymorphism	Reported polymorphism
12S ribosomal RNA	1442	G to A			Reported polymorphism
NADH dehydrogenase 2	4612	T to C	M to T		Reported polymorphism
NADH dehydrogenase 2	5127	A to G	N to D		Reported polymorphism
Cytochrome *c* oxidase 1	6332	A to G	Synonymous		
Cytochrome *c* oxidase 1	7389	C to T	Y to H	Reported polymorphism	
Noncoding nucleotides 7	8272	9bp deletion		Reported polymorphism	
Noncoding nucleotides 7	8291	A to G		Reported polymorphism	Reported polymorphism
NADH dehydrogenase 3	10403	A to G	Synonymous	Reported polymorphism	Reported polymorphism
NADH dehydrogenase 4	11151	C to T	A to V	Reported polymorphism	
NADH dehydrogenase 4	11969	G to A	A to T	Reported polymorphism	
NADH dehydrogenase 5	13105	A to G	I to V	Reported polymorphism	Reported polymorphism
D-loop	16325	T to G			Reported polymorphism
D-loop	16390	G to A		Reported polymorphism	
D-loop	16523	A to G			Reported polymorphism

D-loop = displacement loop; GiiB-JST mtSNP = human mitochondrial genome single nucleotide polymorphism database (http://mtsnp.tmig.or.jp/mtsnp/index.shtml); MITOMAP = human mitochondrial genome database (http://www.mitomap.org); mtDNA = mitochondrial DNA; NADH = reduced nicotinamide adenine dinucleotide.

SDH staining fibers, and CCO-deficient fibers, this case was diagnosed with mitochondrial myopathy.

Muscle biopsy from the other patients revealed several RRFs, highly expressed SDH staining fibers, and CCO-deficient fibers. Histochemical parameters showed relatively mild alterations, and the low frequency of CCO-deficient fibers and RRFs might have been influenced by age-related changes. However, we could not explain the histochemical findings in Cases 8 and 9 as age-related changes because these were younger patients; hence, we surmise that their histochemical findings could be associated with their clinical features and the pathogenetic property of mtDNA alterations. Accordingly, we diagnosed all 9 cases as mitochondrial disease of similar genetic background and clinical findings.

Six patients in this study had experienced severe myalgia at some point in time; this is characteristic of recurrent myoglobinuria associated with mtDNA mutation.[20–22] In contrast, elevated serum CK levels were relatively low in these patients and recurrence rates were also

low; no patient had a history of voiding dark brown urine or acute renal failure. Furthermore, serum CK levels had normalized without medication at follow-up examinations. We believe that mild muscle weakness and the minor, episodic elevation in CK levels observed in our patients could be caused by mitochondrial dysfunction, as indicated by histochemical findings.

Patients in this study originated from 8 different families, but they had the same 16 mtDNA polymorphisms and a similar phenotype. In addition, all patients originated from the southern part of Japan. These results suggest that this disease is of mitochondrial origin, caused by mtDNA alterations, and transmitted by maternal inheritance, leading to the possibility that a common source exists or had existed in southern Japan. At the same time, these mitochondrial diseases were less likely to be associated with nuclear DNA. We evaluated all mtDNA alterations listed in MITOMAP and GiiB-JST (human mitochondrial genome single nucleotide polymorphism database; http://mtsnp.tmig.or.jp/mtsnp/index.shtml), the largest publicly available compendium of mtDNA polymorphisms. We found the following 16 alterations: np200, np257, np1442, np4612, np5127, np6332, np7389, 9bp deletion between np8281 and 8289, np8291, np10403, np11151, np11969, np13105, np16325, np16390, and np16523. However, each alteration previously reported in MITOMAP and GiiB-JST had been described as a nonpathological alteration.

The 16 polymorphisms are probably because of a rare haplotype that is probably derived from the B4f1 haplogroup of the East Asian mtDNA haplogroups that share 14 of the 16 polymorphisms (np200, np257, np1442, np4612, np5127, np6332, np7289, 9bp deletion between np8281 and 8289, np8291, np11969, np13105, np16325, np16390, and np16523).[23]

In addition, oxidative phosphorylation complex activity was studied in a previous study that included 4 of the 9 patients from this study; the activity of complex IV relative to that of citrate synthetase was reduced to about 50% in normal controls in this previous study.[12] Mitochondrial disease is usually caused by a pathological mtDNA rearrangement, with mtDNA mutations being classified as depletion, deletion/duplication, and point mutations. Nevertheless, a previous study reported that retrospective screening of 2,000 patients suspected of mtDNA disorders for common point mutations and large deletions identified mutations in only 6% of the patient population.[24] Mitochondrial myopathies with isolated skeletal muscle involvement and mtDNA mutation are relatively rare. However, many patients could live normally with pure myopathy but still harbor unknown genetic defects in the mtDNA. A previous study reported exercise intolerance due to mutations in the cytochrome *b* gene of mtDNA;[25] the clinical manifestations included progressive exercise intolerance, proximal limb weakness, and in some cases, myoglobinuria.

In several reports, double disease-associated mutations were detected in the same patients with Leber's hereditary optic neuropathy (LHON);[26–28] these mutations may have some influence on the symptoms of LHON. Another study reported that some polymorphisms adjacent to the 3243A>G mutation had different effects on the clinical phenotype, muscle pathology, and respiratory chain enzyme activity.[29] Yet another pathogenesis has been suggested; antiretroviral therapy causes peripheral neuropathy, a pathogenesis in which nucleoside reverse transcriptase inhibitor (NRTI)-associated mitochondrial dysfunction, inflammation, and nutritional factors have been implicated. Owing to its well-documented potential for inducing mitochondrial dysfunction and oxidative stress, NRTI therapy could be considered as a significant environmental challenge, which, when superimposed on genetic susceptibility, leads to a toxicity phenotype. The environmentally determined genetic expression (EDGE) concept provides a framework for considering the combinations of genetic and environmental exposure that define the thresholds for expression of specific phenotypes in an individual. This concept holds that genetic variations in expressed proteins have different effects in different environmental contexts, and that disease or toxicity phenotype is determined by the functional magnitude of the genetic change and the severity of the environmental exposure.[30]

In summary, the findings of distinct clinical features, mitochondrial pathologic changes and the same mitochondrial genetic background in all patients suggest that this disease could be a novel mitochondrial disease. Although we did not identify the key pathogenic mutations, this disease should be associated with some of the 16 mtDNA alterations or at least with their mitochondria. Therefore, we propose that this disease be named as "mitochondrial myopathy with episodic hyper-CK-emia (MIMECK)." We believe that this study provides an insight into a novel aspect of mitochondrial disease pathogenesis.

Furthermore, pharmacogenetic studies on drug-induced and associated mtDNA alterations could contribute to research leading to the discovery and design of novel drugs that would eliminate the negative side effects associated with current therapies. Further genetic and clinical studies, especially involving persons of another race and from other geographic areas, will clarify the pathogenesis of this disease.

Acknowledgments

This research was supported by grants from the Nervous and Mental Disorders and Research Committee for Ataxic Disease of the Japanese Ministry of Health, Welfare and Labor (19A-1 to H.T.); the Ministry of Education, Culture, Sports, Science, and Technology of Japan (21591095 to H.T.; 21591094 to I.H.); and the Nervous and Mental Disorders from the Ministry of Health, Labor, and Welfare (20B-13 to I.H.).

We thank Ms. A. Yoshimura and Ms. N. Hirata of our department for their excellent technical assistance.

Potential Conflict of Interest

I.H. received grants from the Ministry of Education, Culture, Sports, Science, and Technology of Japan (grant 21591094), and the Nervous and Mental Disorders from the Ministry of Health, Labor, and Welfare (grant 20B-13). H.T. received grants from the Nervous and Mental Disorders and Research Committee for Ataxic Disease of the Japanese Ministry of Health, Welfare and Labor (grant 19A-1) and the Ministry of Education, Culture, Sports, Science, and Technology of Japan (grant 21591095). H.T. has received research grants or speaking fees from Eisai, Pfizer, Sanofi-Aventis, Teijin Pharma, Novartis, Tanabe-Mitsubishi Dainippon-Sumitomo, Astellas, GlaxoSmithkline and Benesis.

References

1. Munsat TL, Baloh R, Pearson CM, Fowler W. Serum enzyme alterations in neuromuscular disorders. JAMA 1973;226:1536–1543.
2. Hays AP, Gamboa ET. Acute viral myositis. In: Engel AG, Franzini Armstrong C, eds. Myology: basic and clinical. Vol 2. 2nd ed. New York: McGraw-Hill, 1994;1399–1418.
3. Rowland LP, Willner J, Di Mauro S, Miranda A. Approaches to the membrane theory of Duchenne muscular dystrophy. In: Angelini C, Danieli GA, Fontanri D, eds. Muscular dystrophy-advances and new trends. Amsterdam: Excerpta Medica, 1980;3–13.
4. Joy JL, Oh SJ. Asymptomatic hyper-CK-emia: an electrophysiologic and histopathologic study. Muscle Nerve 1989;12:206–209.
5. Dogue A, Bagheri H. Detection and incidence of muscular adverse drug reactions: a prospective analysis from laboratory signals. Eur J Clin Pharmacol 2004;60:285–292.
6. Baker SK, Tarnopolsky MA. Statin myopathies: pathophysiologic and clinical perspectives. Clin Invest Med 2001;24;258–272.
7. Evans M, Rees A. Effects of HMG-CoA reductase inhibitors on skeletal muscle: are all statins the same? Drug Saf 2002;25: 649–663.
8. Thompson PD, Clarkson P. Statin-associated myopathy. JAMA 2003;289:1681–1690.
9. Dalakas MC. Peripheral neuropathy and antiretroviral drugs. J Peripher Nerv Syst 2001;6:14–20.
10. Brandon MC, Lott MT, Nguyen KC, et al. MITOMAP: a human mitochondrial genome database—2004 update. Nucl Acids Res 2005;33:D611–D613.
11. Dimauro S. Mitochondrial DNA and disease. Ann Med 2005;37: 222–232.
12. Hirata K, Nakagawa M, Higuchi I, et al. Adult onset limb-girdle type mitochondrial myopathy with a mitochondrial DNA np8291 A-to-G substitution. J Hum Genet 1999;44:210–214.
13. Shoffner JM, Lott MT, Lezza AM, et al. Myoclonic epilepsy and ragged-red fiber disease (MERRF) is associated with a mitochondrial DNA tRNA(Lys) mutation. Cell 1990;61:931–937.
14. Maitra A, Cohen Y, Gillespie SE, et al. The human mitochip: a high-throughput sequencing microarray for mitochondrial mutation detection. Genome Res 2004;14:812–819.
15. Zhou S, Kassauei K, Cutler DJ, et al. An oligonucleotide microarray for high-throughput sequencing of the mitochondrial genome. J Mol Diagn 2006;8:476–482.
16. Cutler DJ, Zwick ME, Carraquillo MM, et al. High throughput validation detection and genotyping using microarrays. Genome Res 2001;11:1913–1925.
17. Boerkoel CF, Takashima H, Stankiewicz P, et al. Periaxin mutations cause recessive Dejerine-Sottas neuropathy. Am J Hum Genet 2001;68:325–333.
18. Chariot P, Gherardi R. Myopathy and HIV infections. Curr Opin Rheumatol 1995;7:497–502.
19. Masanes F, Barrientos A, Cebrian M, et al. Clinical, histological and molecular reversibility of zidovudine myopathy. J Neurol Sci 1998;159:226–228.
20. Ohno K, Tanaka M, Sahashi T, et al. Mitochondrial DNA deletions in inherited recurrent myoglobinuria. Ann Neurol 1991;29:364–369.
21. Melberg A, Holme E, Oldfors A, Lundberg PO. Rhabdomyolysis in autosomal dominant progressive external ophthalmoplegia. Neurology 1998;50:299–300.
22. Karadimas CL, Greenstein P, Sue CM, et al. Recurrent myoglobinuria due to a nonsense mutation in the COX I gene of mitochondrial DNA. Neurology 2000;55:644–649.
23. Kong QP, Bandelt HJ, Sun C, et al. Updating the East Asian mtDNA phylogeny: a prerequisite for the identification of pathogenic mutations. Hum Mol Genet 2006;15:2076–2086.
24. Liang MH, Wong L-JC. Yield of mtDNA mutations analysis in 2000 patients. Am J Med Genet 1998;77:385–400.
25. Andreu AL, Hanna MG, Reichmann H, et al. Exercise intolerance due to mutations in the cytochrome b gene of mitochondrial DNA. N Engl J Med 1999;341:1037–1044.
26. Mimaki M, Ikota A, Sato A, et al. A double mutation (G11778A and G121924) in mitochondrial DNA associated with Leber's hereditary optic neuropathy and cardiomyopathy. J Hum Genet 2003;48:47–50.
27. Brown MD, Torroni A, Reckford CL, Wallace DC. Phylogenetic analysis of Leber's hereditary optic neuropathy mitochondrial DNA indicates multiple independent occurrences of the common mutations. Hum Mutat 1995;6:311–325.
28. Riodan-Eva P, Sanders MD, Govan GG, et al. The clinical features of Leber's hereditary optic neuropathy defined by the presence of a pathogenetic mitochondrial DNA mutation. Brain 1995;118:319–337.
29. Mimaki M, Hatakeyama H, Ichiyama T, et al. Different effects of novel mtDNA G3242A and G3244A base changes adjacent to a common A3243G mutation in patients with mitochondrial disorders. Mitochondrion 2009;9:115–122.
30. Kallianpur AR, Hulgan T. Pharmacogenetics of nucleoside reverse-transcriptase inhibitor-associated peripheral neuropathy. Pharmacogenomics 2009;10:623–627.

Optinurin inclusions in proximal hereditary motor and sensory neuropathy (HMSN-P): familial amyotrophic lateral sclerosis with sensory neuronopathy?

Masanori Nakagawa

Proximal hereditary motor and sensory neuropathy (HMSN-P) is an autosomal dominant neuromuscular disease with sensory symptoms that was first described in patients from Okinawa, a southern archipelago in Japan.[1] The clinical features of HMSN-P include proximal dominant neurogenic atrophy with fasciculations, painful muscle cramp, sensory involvement and areflexia. Serum levels of creatine kinase are elevated and patients have a higher incidence of hyperlipidaemia and diabetes mellitus. The electrophysiological findings are consistent with motor and sensory axonal neuropathy. On neuropathological investigation, the sensorimotor neuronopathy is the cardinal feature in HMSN-P. However, brainstem pathology has yet to be elucidated.

HMSN-P is a slowly progressive intractable disease and some patients eventually require a tracheostomy with artificial ventilation, mimicking the clinical course of familial amyotrophic lateral sclerosis (FALS). It is thus no wonder that the dominant differential diagnoses in patients with HMSN-P include FALS, adult onset spinal muscular atrophy (SMA) or Charcot–Marie–Tooth disease type 2. Being an autosomal dominant adult onset disorder, when a patient with HMSN-P is diagnosed, the disease can be transmitted to their next generation, underscoring the need for genetic counselling.

Correspondence to Dr M Nakagawa, Department of Neurology, Graduate School of Medical Science, Kyoto Prefectural University of Medicine, Kawaramachi Hirokoji, Kajii-chou 465, Kamigyo-ku, Kyoto 602-0841, Japan; mnakagaw@koto.kpu-m.ac.jp

The gene locus of HMSN-P has been mapped to an overlapping centromeric region of chromosome 3 in two independent linkage analyses, one from a Okinawa family[1 2] and another from a family from Shiga prefecture in mainland Honshu, Japan.[3]

Fujita and colleagues,[4] proposed that HMSN-P could be considered as a form of FALS with sensory involvement (***see page 1402***), based on the neuropathological findings of brainstem and spinal cord motor neuron involvement with optineurin, which is a new causative gene of FALS reported by Japanese scientists.[5] The clinicopathological features of HMSN-P are similar to those of SOD1 mutated FALS. From the foregoing studies, one may cast some doubt on the classification of this entity as HMSN. While proposed that it might be better regarded as FALS with sensory neuronopathy,[4] the nomenclature of HMSN-P may actually belong to a new subclass under the nosology of ALS.

Maeda *et al* have reported a new case of HMSN-P in a Brazilian family with Japanese ancestry.[6] It is interesting to note that emigration from Japan to Brazil has been widespread since 1908, reaching 18 million at present. In addition, more than one-third of the initial Brazilian immigrants came from the Okinawa islands. The people from the Okinawa prefecture immigrated to the American continents, including Brazil (approximately 130 000), the USA (80 000), Peru (40 000) and other countries (50 000). We can thus assume that HMSN-P is not only limited to Japan, but might have spread worldwide, especially in countries that have received many Okinawan immigrants. Furthermore, it is conceivable that patients with HMSN-P may exist worldwide carrying a diagnosis of FALS, adult onset SMA or Charcot–Marie–Tooth disease type 2.

A number of issues relating to HMSN-P remain to be elucidated, among them the following questions. How is the motor pathology related to the sensory counterpart? What is the causative gene of the disease? How are HMSN-P families in Okinawa and Kansai related? The global epidemiology, pathomechanism and therapeutic strategy for HMSN-P have not been elucidated to date. Because the disease develops usually in the fourth decade of life, mutant genes have a higher chance of transmission to the next generation, underscoring the urgency for seeking the pathomechanism.

The quest for the exact pathomechanism of HMSN-P may contribute to clarification of other neurological diseases, such as FALS and SMA.

Competing interests None.

Provenance and peer review Commissioned; not externally peer reviewed.

Received 21 August 2011
Revised 25 August 2011
Accepted 27 August 2011
Published Online First 23 September 2011

J Neurol Neurosurg Psychiatry 2011;**82**:1299.
doi:10.1136/jnnp-2011-301240

REFERENCES

1. **Takashima H**, Nakagawa M, Nakahara K, *et al*. A new type of hereditary motor and sensory neuropathy linked to chromosome 3. *Ann Neurol* 1997;**41**:771–80.
2. **Takashima H**, Nakagawa M, Suehara M, *et al*. Gene for hereditary motor and sensory neuropathy (proximal dominant form) mapped to 3q13.1. *Neuromuscul Disord* 1999;**9**:368–71.
3. **Maeda K**, Kaji R, Yasuno K, *et al*. Refinement of a locus for autosomal dominant hereditary motor and sensory neuropathy with proximal dominancy (HMSN-P) and genetic heterogeneity. *J Hum Genet* 2007;**52**:907–14.
4. **Fujita K**, Yoshida M, Sako W, *et al*. Brainstem and spinal cord motor neuron involvement with optineurin inclusions in proximal dominant hereditary motor and sensory neuropathy. *J Neurol Neurosurg Psychiatry* 2011;**82**:1402–14.
5. **Maruyama H**, Morino H, Ito H, *et al*. Mutations of optineurin in amyotrophic lateral sclerosis. *Nature* 2010;**465**:223–6.
6. **Maeda K**, Sugiura M, Kato H, *et al*. Hereditary motor and sensory neuropathy (proximal dominant form, HMSN-P) among Brazilians of Japanese ancestry. *Clin Neurol Neurosurg* 2007;**109**:830–2.

Journal of Human Genetics (2011) 56, 341–342

www.nature.com/jhg

COMMENTARY

A Commentary on Molecular diagnosis and clinical onset of Charcot–Marie–Tooth disease in Japan

Masanori Nakagawa

Journal of Human Genetics (2011) **56**, 341–342; doi:10.1038/jhg.2011.32; published online 24 March 2011

The article entitled 'Molecular diagnosis and clinical onset of Charcot-Marie-Tooth disease in Japan' offers new light on the remarkable ethnic diversity of Charcot–Marie–Tooth disease (CMT) in different populations.[1] CMT is indeed the most common inherited peripheral neuropathy. Whereas the prevalence is estimated at one patient per 2500 population in Europe and the United States, the precise prevalence in Japan still remains unexplored. CMT symptoms include an awkward gait, muscular atrophy of the distal extremities and foot deformities (Figure 1). Clinical observations indicate that CMT is highly heterogeneous and may range from patients who may be asymptomatic to those who are bedridden. Thus, CMT may have to be suspected in those patients with peripheral neuropathy and cavus foot, even if no other members of the family have been diagnosed with the disease. This clinical approach will therefore help in framing the precise prevalence and molecular epidemiology of CMT in Japan.

CMT constitutes a genetically heterogeneous group of diseases that affect the peripheral nervous system. Characterized by degeneration or abnormal development of the peripheral nerve and transmitted with different genetic patterns, CMT has been traditionally classified into demyelinating, axonal and intermediate forms based on nerve conduction studies. As for the disease causality, more than 40 genes have been identified (http://www.molgen.ua.ac.be/CMTMutations/Mutations). The proportions of different genotypes in patients with CMT have been reported often in the Caucasian population,[2,3] but rarely in the non-Caucasian population. The authors disclosed the proportions of different genotypes of CMT in the Japanese population, together with 14 novel disease-causing mutations of known CMT genes.[1] This study is a significant genetic survey involving 354 patients with CMT in the non-Caucasian population. They also showed the distinct age of onset in different CMT genes. Most of the patients carrying *PMP22*, *MPZ*, *NEFL*, *PRX* and *MFN2* mutations showed an early disease onset, while half of the patients with *PMP22* duplication and all patients with *GJB1* or *MPZ* mutations showing an axonal phenotype were late disease onset. They also highlighted two epidemiological features in the Japanese population that are distinct from those of the Caucasian population: lower prevalence of duplication of *PMP22* in the demyelinating CMT and more cases in which no causative genes were identified despite an extensive search on the representative CMT genes.[2,3] Arguably, the lower prevalence of *PMP22* duplication in the Japanese population is likely associated with the milder symptoms in this population owing to genetic and/or epigenetic modifying factors. Indeed, a genetic study is essential to identify the causative gene for CMT, to clarify the molecular mechanism of CMT and to pursue the development of novel treatment strategies.

Several questions still remain: How can we ultimately identify the causative genes in the patients with unknown cause? What are the genetic and epigenetic modifying factors that potentially affect the phenotypic expression of patients with *PMP22* duplica-

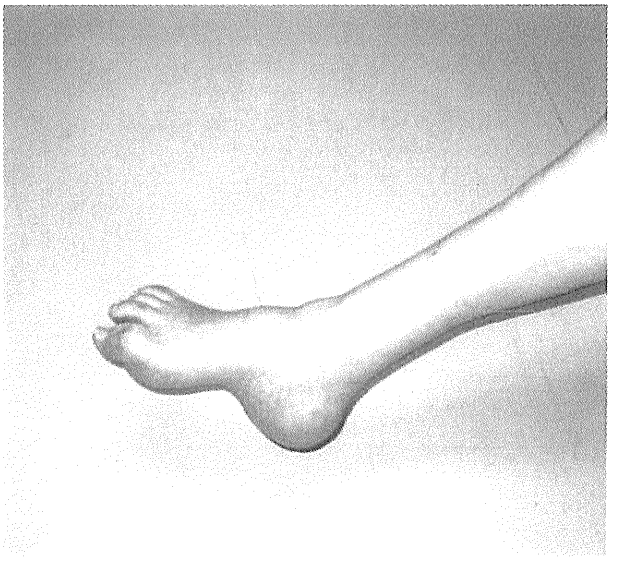

Figure 1 The cavus foot of a CMT patient.

Dr M Nakagawa is at the Department of Neurology, Graduate School of Medical Science, Kyoto Prefectural University of Medicine, Kawaramachi Hirokoji, Kajii-chou 465, Kamigyo-ku, Kyoto 602-0841, Japan.
E-mail: mnakagaw@koto.kpu-m.ac.jp

tion? It could be helpful to establish a high-throughput screening method using the next-generation sequencer for identification of the causative gene of patients with unidentified mutations and the genetic and epigenetic modifying factors of CMT. In addition, a molecular epidemiological study of CMT in Asian countries including Korea and China, where Japanese lineage may encroach, is needed, so as to provide more insight into the genetic background of the low prevalence of *PMP22* duplication in Japan.

1 Abe, A., Numakura, C., Kijima, K., Hayashi, M., Hashimoto, T. & Hayasaka, K. Molecular diagnosis and clinical onset of Charcot-Marie-Tooth disease in Japan. *J. Hum. Genet.* **56,** 364–368 (2011).
2 Mostacciuolo, M. L., Righetti, E., Zortea, M., Bosello, V., Schiavon, F., Vallo, L. *et al.* Charcot-Marie-Tooth disease type I and related demyelinating neuropathies: mutation analysis in a large cohort of Italian families. *Hum. Mutat.* **18,** 32–41 (2001).
3 Boerkoel, C. F., Takashima, H., Garcia, C. A., Olney, R. K., Johnson, J., Berry, K. *et al.* Charcot-Marie-Tooth disease and related neuropathies: mutation distribution and genotype-phenotype correlation. *Ann. Neurol.* **51,** 190–201 (2002).

Citation: Cell Death and Disease (2011) 2, e175; doi:10.1038/cddis.2011.59

www.nature.com/cddis

Axotomy induces axonogenesis in hippocampal neurons through STAT3

R Ohara[1,2], Y Fujita[1,3], K Hata[1], M Nakagawa[2] and T Yamashita[*,1,3]

After axotomy of embryonic hippocampal neurons *in vitro*, some of the axotomized axons lose their identity, and new axons arise and grow. This axotomy-induced axonogenesis requires importin, suggesting that some injury-induced signals are transported via axons to elicit axonogenesis after axotomy. In this study, we show that STAT3 is activated in response to axotomy. Because STAT3 was co-immunoprecipitated with importin β in the axotomized neurons, we suggest that STAT3 is retrogradely transported as molecular cargo of importin α/β heterodimers. Indeed, inhibition of importin α binding with STAT3 resulted in the attenuation of axonogenesis. Silencing STAT3 blocked the axonogenesis, demonstrating that STAT3 is necessary for axotomy-induced axonogenesis. Furthermore, the overexpression of STAT3 enhanced axotomy-induced axonogenesis. Taken together, these results demonstrate that activation and retrograde transport of STAT3 in injured axons have key roles in the axotomy-induced axonogenesis of hippocampal neurons.

Cell Death and Disease (2011) **2**, e175; doi:10.1038/cddis.2011.59; published online 23 June 2011
Subject Category: Neuroscience

The cell body of an injured neuron must receive accurate and timely information about axonal damage to reproduce polarization. It has been widely recognized that a dendrite is transformed into a new axon and that an injured axon regrows after axonal injury.[1,2] In addition to examining these responses, we have focused on the previously unrecognized phenomenon of a new neurite arising from a cell body after axotomy and becoming an axon.[3] In approximately one-tenth of cultured rat hippocampal neurons on embryonic day (E) 18–19, new neurites arise from cell bodies and grow after axotomy (axonogenesis).[3] These neurites become Tau-1 positive, and the injured axons lose immunoreactivity for Tau-1. This axotomy-induced axonogenesis is the third form of response to axonal injury and may be important for plasticity induced by axonal injury. The mechanism underlying this phenomenon has remained a significant question, however.

Because the cell bodies of injured neurons must receive the signals for axonal damage to produce new axons, we reasoned that an injury signal would be transported retrogradely to the cell body by the dynein–dynactin complex. Indeed, axonogenesis can be delayed in these neurons by inhibiting the dynein–dynactin complex through overexpression of p50.[3] Importin β, which is locally translated after axotomy, associates with dynein and is required for axotomy-induced axonogenesis in hippocampal neurons.[3] Importin α protein is constitutively complexed with the retrograde motor dynein; after lesioning, importin β1 mRNA localizes in the axoplasm and is rapidly translated into importin β1 protein, leading to the formation of importin α/β1 heterodimers bound to the retrograde motor dynein.[4] Thus, the axoplasmic importin–dynein complex enables retrograde injury signaling in injured axons. The identification of the molecules that are retrogradely transported is expected to elucidate the mechanism of this interesting phenomenon.

Other studies have identified a number of transcriptional factors in peripheral nerve axons that might be implicated in retrograde signaling,[5] some of which have been reported to interact with importins and their associated molecules for nucleocytoplasmic transport. It is tempting, therefore, to speculate that transcriptional factors interact in axons via importin–dynein-mediated transport as well. Our study showed that STAT3 was activated in response to axotomy and was required for axotomy-induced axonogenesis.

Results

STAT3 inhibitor attenuates axotomy-induced axonogenesis. We cultured hippocampal rat neurons (E18–19) at low density for 3 days and cut the axons of the stage 3 polarized neurons. We then observed morphological changes in these neurons for 12 h using time-lapse imaging. Among 65 axotomized neurons (excluding 10 neurons that died within 3 h of axotomy), axotomized axons regrew in 35 neurons. The remaining dendrites became new axons in 7 neurons, and new neurites arose from the cell bodies after axotomy, grew, and became Tau-1 positive (axonogenesis) in 8 neurons.[3] This axonogenesis was specific to the axotomized neurons, because it was never observed in 62

[1]Department of Molecular Neuroscience, Graduate School of Medicine, Osaka University, 2-2, Yamadaoka, Suita, Osaka 565-0871, Japan; [2]Department of Neurology, Graduate School of Medical Science, Kyoto Prefectural University of Medicine, Kyoto 602-0841, Japan and [3]JST, CREST, 5, Sanbancho, Chiyoda-ku, Tokyo 102-0075, Japan
*Corresponding author: T Yamashita, Department of Molecular Neuroscience, Graduate School of Medicine, Osaka University, 2-2 Yamadaoka, Suita, Osaka 565-0871, Japan. Tel: +81 66 879 3660; Fax: +81 66 879 3669; E-mail: yamashita@molneu.med.osaka-u.ac.jp
Keywords: axonal injury; axonogenesis; STAT3; dynein; importin
Abbreviations: E, embryonic day; NFκB, nuclear factor-κB; NFAT, nuclear factor of activated T cells; DIV, days *in vitro*; pSTAT3, phosphorylated STAT3; TAT-PTD, TAT protein transduction domain; FLC, fluorescein; LIF, leukemia inhibitory factor; CNTF, ciliary neurotrophic factor
Received 07.4.11; revised 17.5.11; accepted 23.5.11; Edited by A Verkhratsky

non-axotomized neurons at the same stage.[3] We assumed that some injury-induced signals would be transported with importin α/β heterodimers and dynein complex from the injury site to the cell body. Therefore, we sought to determine the signal that is transported in the axotomized neurons. STAT3,[6–12] NF-κB,[13–15] nuclear factor of activated T cells (NFAT),[13,16–18] and ERK[19,20] are known molecular cargoes of importin, and they also have roles in axon outgrowth and neuronal survival.

We treated axotomized neurons with membrane-permeable inhibitors AG490 (a STAT3 inhibitor), 6-amino-4-(4-phenoxyphenylethylamino) quinazoline (an inhibitor of NF-κB), U0126 (an inhibitor of ERK), and 11R-vivit (a NFAT inhibitor). AG490 efficiently inhibited axonogenesis but did not modulate the regrowth response (Figure 1a). Although the NF-κB and ERK inhibitors prevented axonogenesis, they also blocked the regrowth response (Figures 1b and c), suggesting that these agents suppress the outgrowth of processes nonspecifically. The NFAT inhibitor did not modulate axotomy-induced axonogenesis (Figure 1d). These results prompted us to focus on the role of STAT3 in axotomy-induced axonogenesis.

STAT3 is activated after axotomy. We tested whether STAT3 was activated after axotomy. The axons of the polarized neurons at 3 days *in vitro* (DIV) were cut and immunostained for phosphorylated STAT3 (pSTAT3) at 10 min, 1, and 3 h after axotomy. The level of pSTAT3 in the nucleus of the axotomized neurons increased significantly at 1 h after axotomy compared with that of non-axotomized neurons (Figures 2a–c). When p50 was transfected with the neurons, however, upregulation of axotomy-induced pSTAT3 in the cell bodies disappeared (Figure 2c).

Next, we evaluated the amount of pSTAT3 in the axotomized neurons. To obtain enough protein for Western blotting, we used an explant culture of the hippocampus from E18 rats. We cut the axons of the hippocampal explants with a blade (Figure 2d) and collected the cell bodies, including the proximal axons and the distal axons (Figure 2e) at 0, 5, 10 min, and 1 h after axotomy. The phosphorylation level of STAT3 was increased after axotomy in both the cell bodies and distal axons (Figures 2e–g). The phosphorylation levels of STAT3 increased gradually up to 10 min after axotomy and remained high even at 1 h after axotomy in the cell bodies and injured the proximal axons (Figures 2e and f). In the distal axons, the level of pSTAT3 peaked 10 min after axotomy and decreased below the baseline 1 h after axotomy (Figures 2e and g). These results demonstrate that pSTAT3 increased in the axons in response to axotomy.

STAT3 is transported through injured axons with importin β. We examined the interaction between pSTAT3 and importin β in axotomized hippocampal neurons. Coimmunoprecipitation analysis revealed that pSTAT3 was associated with importin β1, and this association was

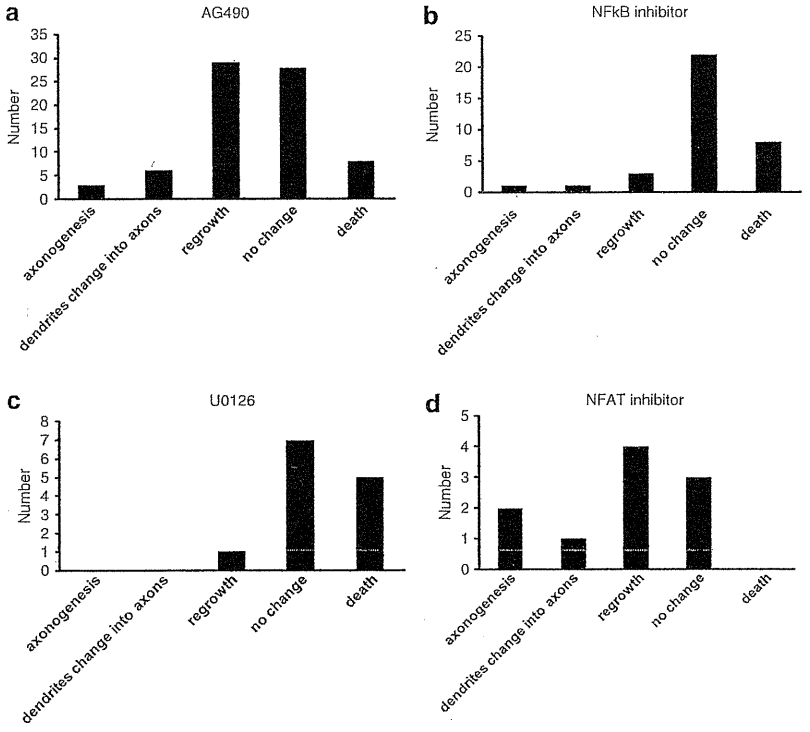

Figure 1 Inhibitor study on axotomy-induced axonogenesis Effects of signal transduction inhibitors on the responses of axotomized hippocampal neurons at 3 DIV. The graphs show the number of neurons with the indicated morphological changes. After axotomy, axonogenesis, but not regrowth of the injured axons, was suppressed by AG490 (**a**; $n=74$). Regrowth as well as axonogenesis was inhibited by treatment with NFκB inhibitor (**b**; $n=35$) or U0126 (**c**; $n=13$). No significant effect was observed with NFAT inhibitor (**d**; $n=10$)

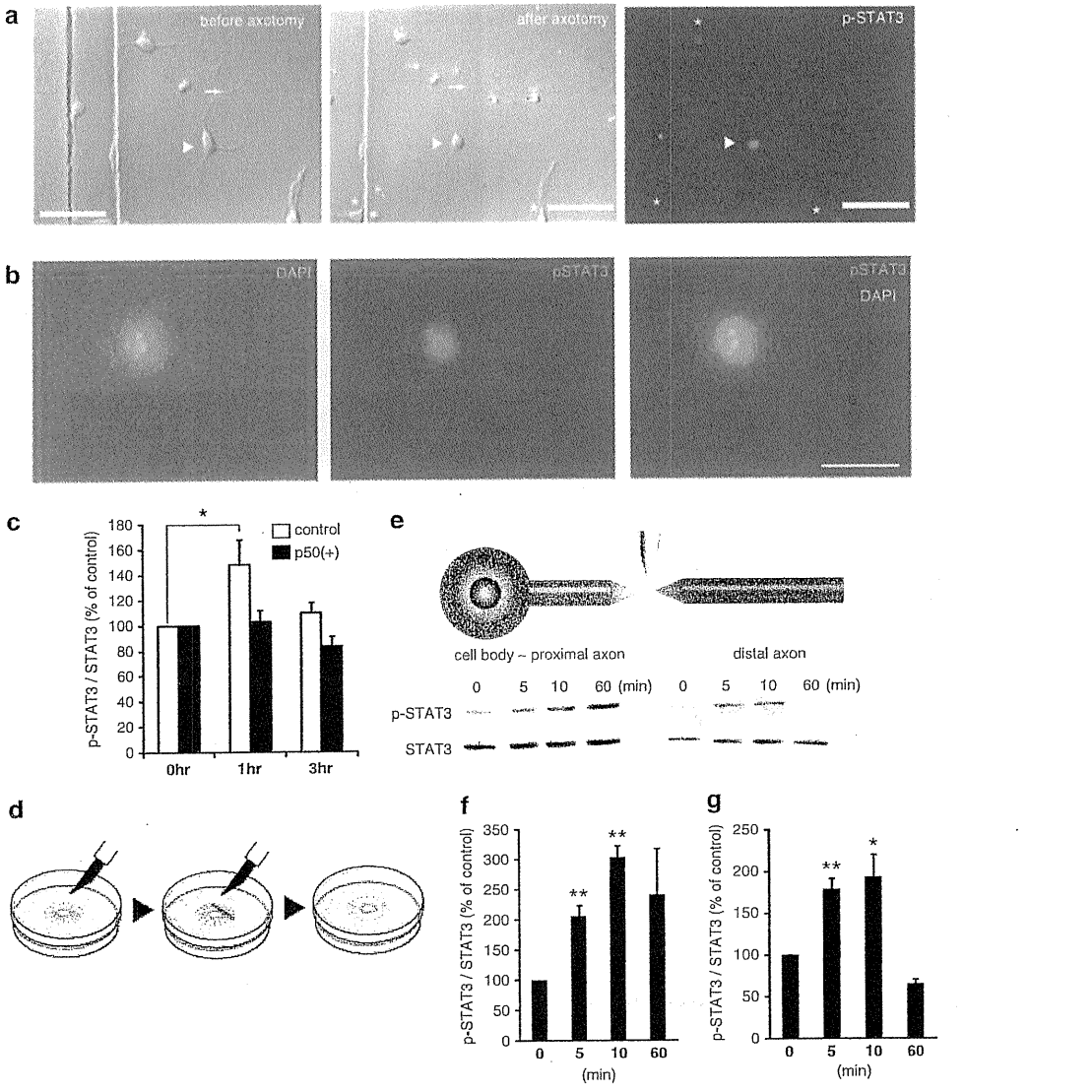

Figure 2 STAT3 is required for axotomy-induced axonogenesis (**a**) Immunocytochemistry for phosphorylated STAT3 (pSTAT3) before and at 1 h after axotomy. pSTAT3 was increased in the nuclei of axotomized hippocampal neurons (arrowhead) compared with the non-axotomized neurons (asterisks). Arrows indicate the injury site, and arrowheads indicate the cell bodies of axotomized neurons. Scale bar, 50 μm. (**b**) The hippocampal neurons were double-immunostained for pSTAT3 (red) and DAPI (blue). pSTAT3 was expressed in the nucleus of the neurons after axotomy. Scale bar, 20 μm. (**c**) Relative level of pSTAT3 in the nucleus. The level of pSTAT3 in the nucleus of axotomized neurons increased significantly at 1 h after axotomy but returned to the control level 3 h after axotomy. In cells with p50 overexpression, the level of pSTAT3 in the nucleus did not increase at 1 or 3 h after axotomy (each group, $n=13$–15). The ratio of pSTAT3/STAT3 was calculated from the fluorescent intensities in immunocytochemistry. Data are represented as mean ± S.E.M. $^*P<0.05$. (**d**) Procedure for transfection of neurites from the explant. (**e**) Western blot analysis of lysates from axotomized hippocampal explants from 0 min to 1 h after axotomy. Lysates were obtained from the cell bodies that included the proximal axons as well as from the distal axons. (**f** and **g**) Relative changes in the level of pSTAT3. The level of pSTAT3 increased at 5 and 10 min after axotomy in both tissues. The ratio was obtained by measuring the band intensities. In the cell bodies and proximal axons (**f**), the increase was gradual and remained high 60 min after axotomy. In the distal axons (**g**), the increase peaked at 10 min after axotomy and decreased dramatically thereafter. Data are represented as the mean ± S.E.M. of three independent experiments. $^{**}P<0.01$; $^*P<0.05$ compared with control

increased at 1 h after axotomy (Figure 3a). We have reported that importin β increases in axons in response to axotomy and that they interact with the dynein motor complex for retrograde transport.[3] These results suggest that pSTAT3 interacts with dynein–importin α/β heterodimers for retrograde transport.

We then attempted to assess whether the binding of STAT3 with importin α/β heterodimers was required for axotomy-induced axonogenesis. Because Arg214/215 of STAT3 is the binding site for importin α5,[7,21] we intended to block the binding of STAT3 with importin α5 specifically by using STAT3, a 10-amino-acid residue peptide (210–219) that includes the binding site of STAT3 with importin α5. This peptide was fused with the amino (N)-terminal protein transduction domain (11 amino acids) from the HIV protein TAT-protein transduction domain (TAT-PTD) and conjugated with fluorescein (FLC) to produce FLC-TAT-PTD-STAT3 (210–219). We used immunocytochemistry to confirm that

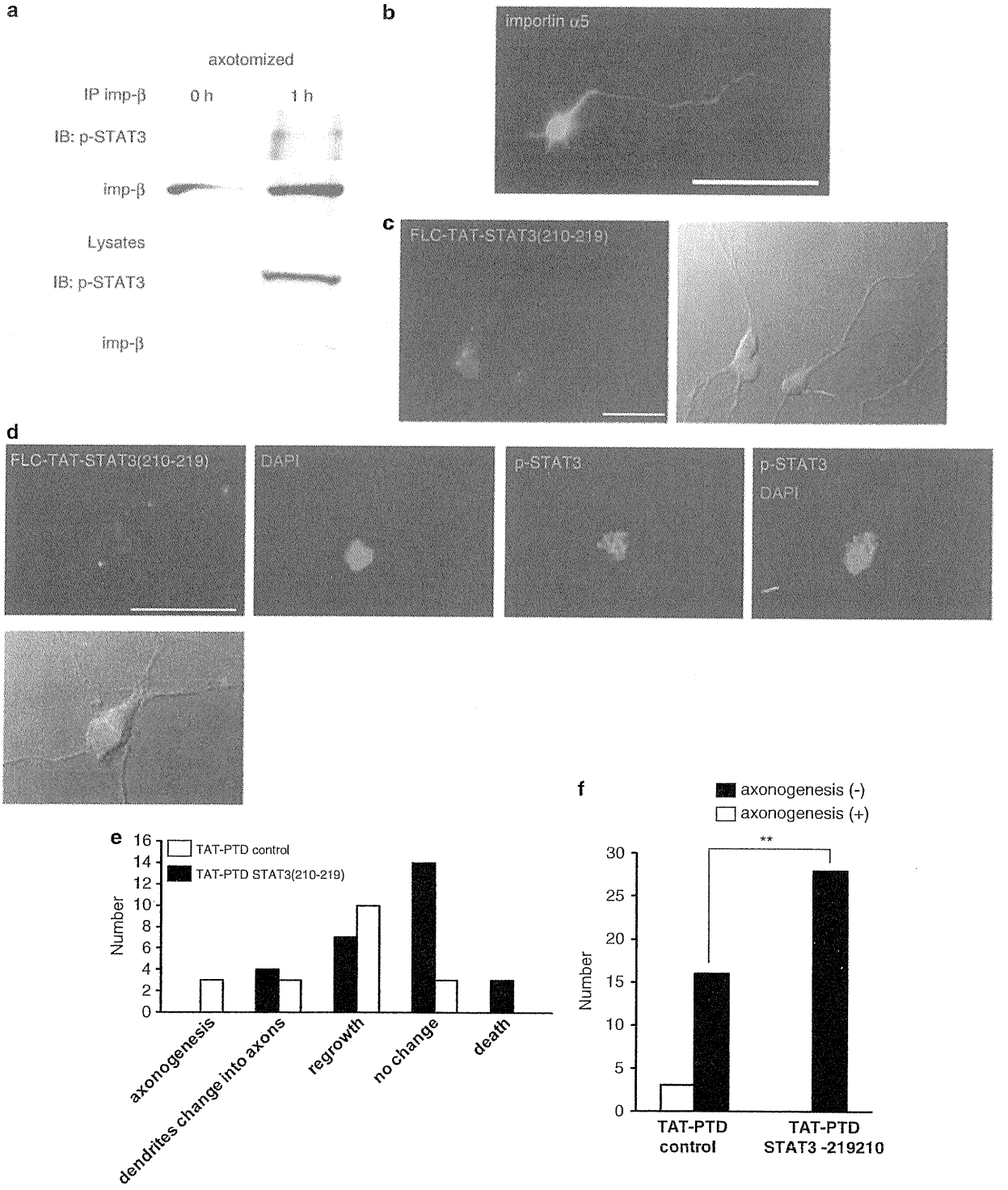

Figure 3 STAT3 binding to importin is required for axotomy-induced axonogenesis (**a**) Coimmunoprecipitation of importin β1 with pSTAT3. Lysates were prepared from hippocampal explants at 1 h after axotomy. (**b**) Immunostaining of a hippocampal neuron at 3 DIV reveals expression of importin α5. Scale bar, 50 μm. (**c**) Fluorescein-TAT-protein transduction domain-STAT3 (FLC-TAT-PTD-STAT3) (210–219) was efficiently transduced in the hippocampal neurons. Scale bar, 50 μm. (**d**) The hippocampal neurons were double-immunostained for pSTAT3 (red) and DAPI (blue). pSTAT3 was expressed in the cytoplasm, but not in the nucleus in the neurons transduced with FLC-TAT-PTD-STAT3 (210–219). Scale bar, 30 μm. (**e**) Number of neurons with the indicated morphological changes. No axonogenesis occurred after axotomy in the neurons transduced with FLC-TAT-PTD-STAT3 (210–219) ($n=28$). TAT-PTD control neurons, $n=16$. (**f**) Number of neurons with and without axonogenesis. Axonogenesis was attenuated in neurons transduced with TAT-PTD STAT3 (210–219), but not in those transduced with TAT-PTD control. $^{**}P<0.05$

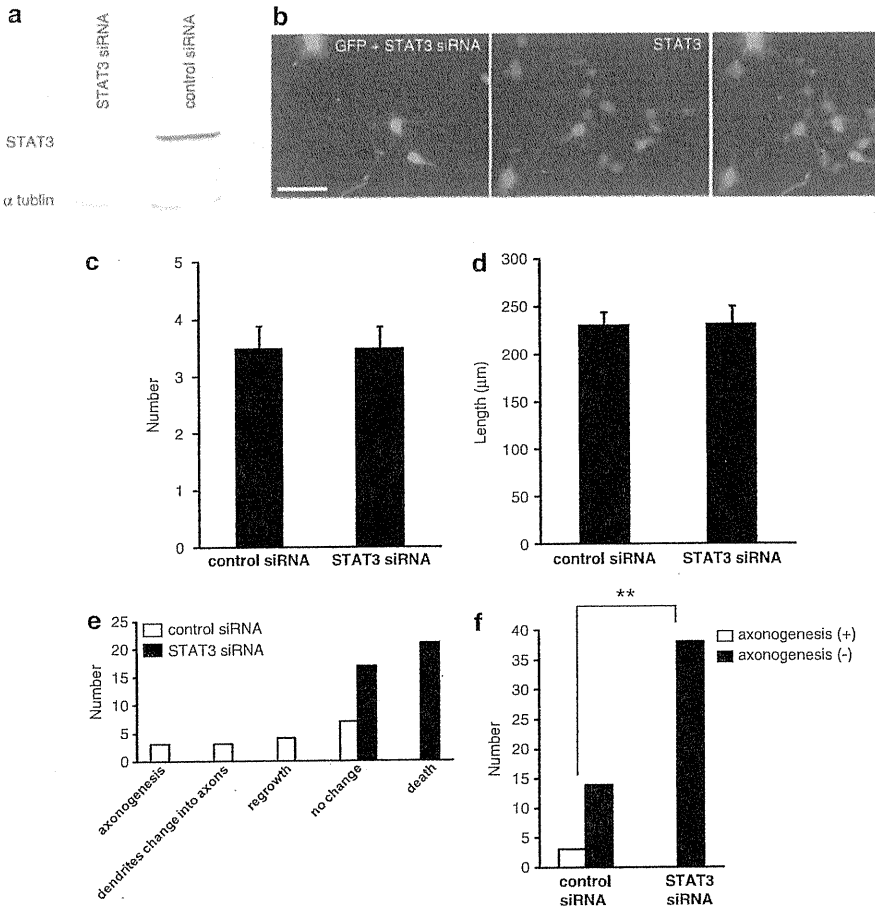

Figure 4 STAT3 is required for axotomy-induced axonogenesis. (**a**) Western blot analysis for the detection of STAT3. The hippocampal neurons at 3DIV were cotransfected with STAT3 siRNA or control siRNA in combination with GFP. (**b**) Immunostaining for STAT3 shows that the expression of STAT3 decreased in the STAT3 siRNA-transfected neurons compared to non-transfected neighboring neurons. Scale bar, 50 μm. (**c**) Number of neurites. Cultured hippocampal neurons were transfected with STAT3 siRNA ($n=23$) or control siRNA ($n=20$). Data are represented as mean ± S.E.M. (**d**) Axonal length. Data are represented as mean ± S.E.M. (**e**) Number of neurons with the indicated morphological changes. No axonogenesis occurred after axotomy in the neurons transfected with STAT3 siRNA ($n=38$). Control siRNA, $n=17$. (**f**) Number of neurons with and without axonogenesis. Knockdown of STAT3 inhibited axonogenesis. $^{**}P<0.01$

importin α5 was expressed in rat hippocampal neurons (Figure 3b). In the dissociated culture of the hippocampal neurons, we transduced FLC-TAT-PTD-STAT3 (210–219) (Figure 3c). Immunocytochemical data revealed that the signal for pSTAT3 was absent in the nuclei of neurons transduced with FLC-TAT-PTD-STAT3 (210–219), demonstrating that the binding of STAT3 with importin α5 was blocked successfully by transduction of FLC-TAT-PTD-STAT3 (210–219) (Figure 3d). By transducing this peptide, we attenuated injury-induced axonogenesis completely (Figures 3e and f). Thus, the binding of STAT3 with importin α5 is required for axotomy-induced axonogenesis.

STAT3 is required for the axotomy-induced axonogenesis. We next investigated the role of STAT3 in axotomy-induced axonogenesis by knocking down its endogenous expression in cultured hippocampal neurons. Nucleofection with the STAT3 siRNA construct, but not with the control siRNA construct, decreased STAT3 expression in the hippocampal neurons at 3 DIV (Figure 4a). We performed nucleofection of the STAT3 siRNA construct in combination with the GFP construct to visualize the transfected neurons (Figure 4b). We transected the axons of the transfected neurons and found that neurons transfected with STAT3 siRNA did not have a significantly different number of processes (Figure 4c) or axonal length (Figure 4d) compared with those transfected with control siRNA. Thus, STAT3 is not involved in the neuritogenesis or the elongation of the processes of uninjured neurons. We observed no axonogenesis after axotomy in the 38 STAT3 siRNA-transfected neurons, however (Figures 4e and f). Thus, STAT3 appears to be necessary for axotomy-induced axonogenesis.

Overexpression of STAT3 promotes axotomy-induced axonogenesis. We transfected Flag-tagged STAT3 construct in combination with GFP into the cultured hippocampal neurons. We verified that almost all of the

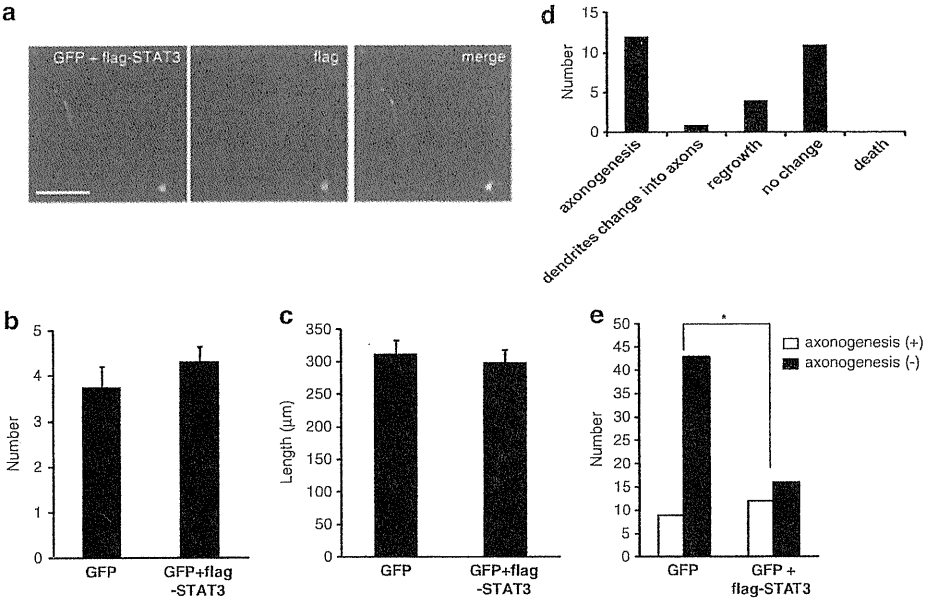

Figure 5 Overexpression of STAT3 enhances axotomy-induced axonogenesis. (**a**) Cultured hippocampal neurons at 3 DIV were transfected with Flag-STAT3 and GFP. Scale bar, 50 μm. (**b**) Number of neurites. Cultured hippocampal neurons were transfected with GFP ($n=25$) or GFP plus Flag-STAT3 ($n=28$). Data are represented as mean ± S.E.M. (**c**) Axonal length. Data are represented as mean ± S.E.M. (**d** and **e**) Axonogenesis after axotomy was increased in the neurons expressing GFP plus Flag-STAT3 ($n=28$). GFP, $n=52$. $^*P<0.05$

GFP-expressing neurons also expressed Flag-tagged STAT3 (Figure 5a). Neurons overexpressing STAT3 showed no significant difference in the number of processes (Figure 5b) or in axonal length (Figure 5c) compared with those of neurons expressing GFP alone. Interestingly, axonogenesis after axotomy occurred in 12 out of 28 STAT3-overexpressed neurons, whereas the same occurred in 9 out of 52 neurons expressing GFP alone (Figures 5d and e), which indicates that axotomy-induced axonogenesis is enhanced by the overexpression of STAT3. These results demonstrate that STAT3 accelerates axotomy-induced axonogenesis.

Discussion

In this study, we have shown that STAT3 is involved in axonogenesis after axotomy. STAT3 is activated in response to axotomy and is transported with importin β through the injured axons. STAT3 is required specifically for the axotomy-induced axonogenesis, and overexpression of STAT3 promotes this event.

Accumulated evidence suggests that STAT3 participates in the responses of injured neurons *in vitro* and *in vivo*. It has been reported previously that axotomy increases pSTAT3 in the sciatic nerve.[9,22,23] Moreover, pSTAT3 has been shown to be transported retrogradely from an injury site to the cell body after sciatic nerve, facial nerve, and hypoglossal nerve lesioning.[24] STAT3 is activated in injured sensory neurons, and the application of a JAK inhibitor attenuates the injury response *in vitro*.[25] Further, *in vivo* peripheral nerve lesioning has been demonstrated to lead to a very rapid activation of STAT3 in sciatic nerve axons at the lesion site.[22] This response increases during the first 24 h after injury and extends back to cell bodies over a time course consistent with that required for the retrograde transport of activated STAT3 from injury site to cell body.[22] The phosphorylation of STAT3 and its translocation from cytoplasm to the nuclei of DRG neurons and motor neurons are increased after injury,[9,24] and STAT3 has been reported to interact with a number of importins.[6,8] Taken together, these findings suggest that STAT3 is retrogradely transported to elicit responses to axonal lesioning. Although STAT3 regulates a wide variety of responses in neurons, the present study is the first to demonstrate that it is involved in axonogenesis. Intriguingly, the data suggest that STAT3 is not a global regulator of axonogenesis but is specifically associated with injury-induced axonogenesis.

Axonogenesis after axotomy was specifically suppressed in neurons transfected with STAT3 siRNA, as the siRNA transfection had no effect on the number of processes or the axonal elongation of uninjured cells. STAT3 is activated in response to growth factors, cytokines, and hormones known to have a protective role after cerebral ischemia and nerve injury.[26–28] Schweizer *et al*[12] used a tissue-specific gene ablation of STAT3 in motor neurons to study the role of neural STAT3 in nerve injury in adults and reported that STAT3 contributes to motor neuron protection after injury-induced neuronal death. Naturally occurring motor neuron death during the embryonic period was not enhanced in neurofilament light chain promoter–Cre STAT3-knockout mice. Facial motor neuron survival was significantly reduced in these mice after nerve lesioning in adults, however. This result suggests that STAT3 has an important role in promoting neuronal survival after injury. Consistent with this observation, knockdown of STAT3 increased neuronal death after axotomy in our study. Because more than half of the STAT3

siRNA-transfected neurons died within 6 h after axotomy, STAT3 appears to be necessary for cells to survive axotomy. Hence, STAT3 contributes to survival and axonogenesis in axotomized neurons.

The neuropoietic cytokines IL-6, leukemia inhibitory factor (LIF), and ciliary neurotrophic factor (CNTF), which are known to be induced after ischemia and nerve injury and which exert neuroprotective and regenerative effects,[27,29–33] share the signaling receptor gp130. In peripheral nerves, CNTF is stored in the cytoplasm of Schwann cells and may be released by injury.[34–38] LIF and IL-6 are present at very low levels in the nerve as well.[39–42] After experimental axonal injury, IL-6 was synthesized in cortical, thalamic, and hippocampal neurons.[43] Although STAT3 was phosphorylated in axotomized neurons, it remains unknown which ligand phosphorylated STAT3 after axonal injury. Because we used dissociated cultures of hippocampal neurons in this study, we assumed that the injured neurons themselves produced some ligand, such as IL-6, CNTF, or LIF, that activated STAT3 or that they induced STAT3 activation independent of any ligand.

The *in vivo* relevance of our observations is an issue to be addressed in the future. *In vivo* synaptic plasticity in the formation of new circuits through collateral sprouting of injured axons is an important component of the functional recovery process in patients with central nervous system injury.[44,45] These reorganization processes possibly occur in cortical and subcortical motor areas. Whether axonogenesis occurs and has a role in recovery after central nervous system injury, such as traumatic brain injury and spinal cord injury is unknown, however. The next challenge will be to explore whether new axons arise *in vivo* from cell bodies of neurons after these injuries.

Materials and Methods

Dissociated cell culture. All experimental procedures were approved by the Institutional Ethics Committee of Osaka University. Hippocampal neurons obtained from Wistar rat pups on E18–19 were dissociated using trypsinization (treatment with 0.25% trypsin in PBS for 15 min at 37 °C) and then resuspended in DMEM/F12 (Invitrogen, Carlsbad, CA, USA) containing 10% FBS and triturated. Subsequently, the neurons were washed three times. The cells were suspended in DMEM/F12 containing 10% FBS, plated on poly-L-lysine- and laminin-coated dishes, and maintained at 37 °C in 5% CO_2. The culture medium was replaced with serum-free DMEM/F12 supplemented with B27 (Invitrogen) at 12 h after plating, by when the cells had attached. For the immunocytochemistry experiments to detect pSTAT3, cells were suspended in DMEM/F12 containing 3% FBS, and the culture medium was replaced with serum-free DMEM/F12 supplemented with B27 at 12 h after plating because the level of pSTAT3 in hippocampal neurons is increased by serum. Where indicated, the following reagents were used at the indicated concentrations: 50 μM AG490 (a STAT3 inhibitor; Calbiochem, San Diego, CA, USA), 50 nM 6-amino-4-(4-phenoxyphenylethylamino) quinazoline (an inhibitor of nuclear factor-κB [NF-κB]; Calbiochem), 10 μM U0126 (an inhibitor of ERK; Calbiochem), 1 μM 11R-vivit (RRRRRRRRRRR-GGG-MAGPHPVIVITGPHEE, an inhibitor of NFAT; Calbiochem). Cells were pretreated with each inhibitor for 30 min before axotomy.

Explant culture. The hippocampus was removed from Wistar rat pups on E18 according to a previously reported method, with slight modification.[46] The hippocampus was chopped into 300- to 600-μm pieces using fine tweezers. These pieces were placed in a 3.5-cm tissue culture dish containing DMEM/F12, 1.5 ml and supplemented with 10% FBS. After 2 days of incubation at 37 °C in a 5% CO_2 incubator, the medium was replaced with DMEM/F12 supplemented with 2% B27. At 10 DIV, the extended neurites were transected with a blade, according to a previously reported method.[47]

Nucleofection procedure. For each transfection experiment, 4.0–5.0 $\times$ 10^6 cells were used with the Nucleofector II device (Amaxa Biosystems, Köln, Germany). Dissociated hippocampal neurons were spun at 800 r.p.m. for 3 min, and the medium was removed. Cells were then resuspended in 100 μl of rat neuron Nucleofector solution (Amaxa Biosystems) at RT, and 5 μg of plasmids were added, including GFP-expression vector (Amaxa Biosystems) and Flag-STAT3-C Flag pRc/CMV (Addgene, Cambridge, MA, USA) at the ratio of 1 : 10. The mixture of neurons, solution, and plasmids was transferred to a 2-mm electroporation cuvette (Amaxa Biosystems), inserted into the Nucleofector, and processed with program O-03. Immediately after transfection, 1 mL of DMEM/F12 supplemented with 10% FBS was added to the hippocampal neurons to reduce damage, and the cells were plated on poly-L-lysine- and laminin-coated dishes. The culture medium was replaced with serum-free DMEM/F12, supplemented with B27 at 3 h after plating to reduce damage to the cells. To knockdown the expression of STAT3, the neurons were cotransfected with 500 pmol of rat STAT3 siRNA (5′-CCACUCUGGUGUUU CAUAACCUCUU-3′) (Stealth Select RNAi; Invitrogen) or control siRNA (Stealth RNAi Negative Control Low GC Duplex; Invitrogen) in combination with 2.5 μg of GFP-plasmid (Amaxa Biosystems). The number of processes and axonal length of the neurons were measured at 48 h after nucleofection.

Axotomy and time-lapse imaging. The culture dish was secured in a chamber that was supplied continuously with 5% CO_2 in air. The chamber was placed on an Olympus IX81 inverted phase-contrast microscope equipped with a heated stage apparatus (model MI-IBC-IF; Olympus, Tokyo, Japan). We chose 10–15 polarized hippocampal neurons in each dish at 3 DIV and cut the axons of the neurons using a 30-G needle through the microscope. Images of the axotomized neurons were acquired every 3 min for 12 h using a $\times$ 40 objective lens with a charge-coupled device video camera (Cooke, Kelheim, Germany). Images were combined into a time-lapse sequence using the MetaMorph software (Molecular Devices, Sunnyvale, CA, USA).

Transduction of TAT–PTD fusion protein. FLC—TAT–PTD (YGRKKRRQRRR)-STAT3 210–219 (LDQMRRSIVS) fusion peptide and FLC–TAT–PTD (YGRKKRRQRRR)–(SRQLVMRDIS) fusion peptide (control) were synthesized by Sigma Genosys (Ishikari, Japan). The peptides, which were purified using preparative reverse-phase HPLC, displayed >95% purity. Hippocampal neurons were incubated with 5 μmol FLC–TAT–PTD-STAT3 210–219 or FLC–TAT–PTD in serum-free DMEM/F12 supplemented with B27 for 3 h at 3 DIV. Subsequently, the neurons were washed with PBS, and the culture medium was replaced with serum-free DMEM/F12 supplemented with B27. The treated neurons were observed for 12 h after axotomy using time-lapse imaging.

Fluorescence immunostaining. Cells were fixed in 2% paraformaldehyde and 2% sucrose in 0.1 mol phosphate buffer for 20 min at RT. They were incubated with a blocking solution containing 5% BSA and 0.1% Triton-X in PBS for 1 h and overnight at 4 °C with anti-importin α5 (diluted 1 : 100 in the blocking solution; Sigma-Aldrich, St. Louis, MO, USA), anti-phospho STAT3 (Ty705) antibody (diluted 1 : 500 in the blocking solution; Cell Signaling Technology, Danvers, MA, USA), anti-STAT3 (124H6) mouse monoclonal antibody (diluted 1 : 500 in the blocking solution; Cell Signaling Technology), and anti-FLAG antibody (diluted 1 : 1000 in the blocking solution; Sigma-Aldrich). After primary antibody incubation, sections were washed three times with PBS and incubated with 1 μg/ml DAPI and fluorescent dye Alexa 488-conjugated anti-rabbit IgG or 568-conjugated anti-mouse IgG (diluted 1 : 1000 in 5% BSA in PBS; Molecular Probes/Invitrogen) at RT for 1 h. They were then observed with an Olympus IX81 inverted phase-contrast microscope.

Western blotting. Cells were lysed using a mixture containing 50 mmol Tris-HCl (pH 7.4), 150 mM NaCl, 1% Np-40, 0.1% SDS, 2 mmol EDTA, 1 mmol Na3VO4, 1 mmol NaF, and a protease inhibitor (Roche Diagnostics, Indianapolis, IN, USA). The homogenate was centrifuged at 15 000 r.p.m. for 10 min, and the supernatant was stored at −20 °C. The protein concentration was measured using a bicinchoninic acid protein assay kit (Pierce; Thermo Fisher Scientific, Rockford, IL, USA). An equal amount of the protein was loaded into each lane, run on SDS-PAGE, and transferred to a PVDF membrane (Millipore, Billerica, MA, USA). The protein samples were boiled in sample buffer for 5 min, run on SDS-PAGE, and transferred to PVDF membranes (Millipore). The membranes were blocked for 1 h at RT with 5% BSA and incubated for 2 h at RT with anti-phospho STAT3(Ty705) antibody (diluted 1 : 1000; Cell Signaling Technology) or anti-STAT3(124H6) antibody (diluted 1 : 500; Cell Signaling Technology). HRP-conjugated secondary

antibodies (diluted 1 : 1000; Cell Signaling Technology) and ECL Plus reagents (GE Healthcare, London, UK) were used for detection. The membrane was exposed to X-ray film or the LAS-3000 image system (Fujifilm, Tokyo, Japan), according to the manufacturer's specifications.

Coimmunoprecipitation assay. Rat hippocampal explants were lysed in 50 mol Tris-HCl (pH 7.5), 150 mmol NaCl, 10% glycerol, and 1% NP-40 supplemented with protease inhibitor cocktail tablets (Roche Diagnostics). The lysates were incubated on a rocking platform at 4 °C for 20 min and clarified by centrifugation at 13 000 × *g* at 4 °C for 10 min. The supernatants were precleared for 30 min by incubating with 60 μl of protein-G Sepharose beads (GE Healthcare). After a brief centrifugation to remove the precleared beads, the cell lysates were incubated overnight (for coimmunoprecipitation with rat hippocampal explants extracts) at 4 °C with anti-importin β antibody (Abcam, Cambridge, MA, USA). The immunocomplexes were collected for 1 h at 4 °C with protein-G Sepharose beads coated with 0.1% BSA in PBS. The beads were washed four times with lysis buffer. The bound proteins were solubilized with × 2 sample buffer and subjected to SDS-PAGE followed by immunoblotting.

Morphometric analysis. We classified the morphological changes of axotomized neurons into five groups as follows: axonogenesis, new neurites that arose from cell bodies after axotomy and grew; dendrites that changed into axons, dendrites that grew and became axons instead of axotomized axons; regrowth, axotomized axons that regrew; no change, axotomized axons that retracted or showed no morphological change; and death, neurons died within 3 h of axotomy. We performed immunocytochemistry for Tau-1 in the first set of experiments, and confirmed that all the new neurites that arose from cell bodies after axotomy and grew were axons.[3]

For the quantification of neurite outgrowth, images were captured on an Olympus IX81 inverted phase-contrast microscope mounted with a charge-coupled device video camera (Cooke, Leicester, UK) using a × 20 objective lens. Analysis was performed using MetaMorph software (Molecular Devices). Twenty to twenty-eight neurons per well were analyzed. Processes were defined as neurites that emerged from the cell body, and an axonal length was defined as the length of the longest neurite.

Statistical analysis. Significant differences in the data for axonogenesis after axotomy (Figures 3f, 4f and 5e) were determined using the χ^2-test. Significant differences in other data were determined using Scheffe's multiple comparison tests. A P-value < 0.05 was considered significant.

Conflict of Interest

The authors declare no conflict of interest.

Acknowledgements. This study was supported by a Grant-in-Aid for Young Scientists (S) from the Japan Society for the Promotion of Science.

1. Dotti CG, Banker GA. Experimentally induced alteration in the polarity of developing neurons. *Nature* 1987; **330**: 254–256.
2. Gomis-Ruth S, Wierenga CJ, Bradke F. Plasticity of polarization: changing dendrites into axons in neurons integrated in neuronal circuits. *Curr Biol* 2008; **18**: 992–1000.
3. Ohara R, Hata K, Yasuhara N, Mehmood R, Yoneda Y, Nakagawa M *et al.* Axotomy induces axonogenesis in hippocampal neurons by a mechanism dependent on importin β. *Biochem Biophys Res Commun* 2011; **405**: 697–702.
4. Hanz S, Perlson E, Willis D, Zheng JQ, Massarwa R, Huerta JJ *et al.* Axoplasmic importins enable retrograde injury signaling in lesioned nerve. *Neuron* 2003; **40**: 1095–1104.
5. Abe N, Cavalli V. Nerve injury signaling. *Curr Opin Neurobiol* 2008; **18**: 276–283.
6. Liu L, McBride KM, Reich NC. STAT3 nuclear import is independent of tyrosine phosphorylation and mediated by importin-alpha3. *Proc Natl Acad Sci USA* 2005; **102**: 8150–8155.
7. Ma J, Cao X. Regulation of Stat3 nuclear import by importin alpha5 and importin alpha7 via two different functional sequence elements. *Cell Signal* 2006; **18**: 1117–1126.
8. Ushijima R, Sakaguchi N, Kano A, Maruyama A, Miyamoto Y, Sekimoto T *et al.* Extracellular signal-dependent nuclear import of STAT3 is mediated by various importin alphas. *Biochem Biophys Res Commun* 2005; **330**: 880–886.
9. Qiu J, Cafferty WB, McMahon SB, Thompson SW. Conditioning injury-induced spinal axon regeneration requires signal transducer and activator of transcription 3 activation. *J Neurosci* 2005; **25**: 1645–1653.
10. Dziennis S, Jia T, Ronnekleiv OK, Hurn PD, Alkayed NJ. Role of signal transducer and activator of transcription-3 in estradiol-mediated neuroprotection. *J Neurosci* 2007; **27**: 7268–7274.
11. Okada S, Nakamura M, Katoh H, Miyao T, Shimazaki T, Ishii K *et al.* Conditional ablation of Stat3 or Socs3 discloses a dual role for reactive astrocytes after spinal cord injury. *Nat Med* 2006; **12**: 829–834.
12. Schweizer U, Gunnersen J, Karch C, Wiese S, Holtmann B, Takeda K *et al.* Conditional gene ablation of Stat3 reveals differential signaling requirements for survival of motoneurons during development and after nerve injury in the adult. *J Cell Biol* 2002; **156**: 287–297.
13. Torgerson TR, Colosia AD, Donahue JP, Lin YZ, Hawiger J. Regulation of NF-kappa B, AP-1, NFAT, and STAT1 nuclear import in T lymphocytes by noninvasive delivery of peptide carrying the nuclear localization sequence of NF-kappa B p50. *J Immunol* 1998; **161**: 6084–6092.
14. Mattson MP, Culmsee C, Yu Z, Camandola S. Roles of nuclear factor kappaB in neuronal survival and plasticity. *J Neurochem* 2000; **74**: 443–456.
15. Fagerlund R, Kinnunen L, Kohler M, Julkunen I, Melen K. NF-{kappa}B is transported into the nucleus by importin {alpha}3 and importin {alpha}4. *J Biol Chem* 2005; **280**: 15942–15951.
16. Graef IA, Mermelstein PG, Stankunas K, Neilson JR, Deisseroth K, Tsien RW *et al.* L-type calcium channels and GSK-3 regulate the activity of NF-ATc4 in hippocampal neurons. *Nature* 1999; **401**: 703–708.
17. Willingham AT, Orth AP, Batalov S, Peters EC, Wen BG, Aza-Blanc P *et al.* A strategy for probing the function of noncoding RNAs finds a repressor of NFAT. *Science* 2005; **309**: 1570–1573.
18. Benedito AB, Lehtinen M, Massol R, Lopes UG, Kirchhausen T, Rao A *et al.* The transcription factor NFAT3 mediates neuronal survival. *J Biol Chem* 2005; **280**: 2818–2825.
19. Whitehurst AW, Wilsbacher JL, You Y, Luby-Phelps K, Moore MS, Cobb MH. ERK2 enters the nucleus by a carrier-independent mechanism. *Proc Natl Acad Sci USA* 2002; **99**: 7496–7501.
20. Perlson E, Hanz S, Ben-Yaakov K, Segal-Ruder Y, Seger R, Fainzilber M. Vimentin-dependent spatial translocation of an activated MAP kinase in injured nerve. *Neuron* 2005; **45**: 715–726.
21. Sato N, Tsuruma R, Imoto S, Sekine Y, Muromoto R, Sugiyama K *et al.* Nuclear retention of STAT3 through the coiled-coil domain regulates its activity. *Biochem Biophys Res Commun* 2005; **336**: 617–624.
22. Lee N, Neitzel KL, Devlin BK, MacLennan AJ. STAT3 phosphorylation in injured axons before sensory and motor neuron nuclei: potential role for STAT3 as a retrograde signaling transcription factor. *J Comp Neurol* 2004; **474**: 535–545.
23. Sheu JY, Kulhanek DJ, Eckenstein FP. Differential patterns of ERK and STAT3 phosphorylation after sciatic nerve transection in the rat. *Exp Neurol* 2000; **166**: 392–402.
24. Schwaiger FW, Hager G, Schmitt AB, Horvat A, Hager G, Streif R *et al.* Peripheral but not central axotomy induces changes in Janus kinases (JAK) and signal transducers and activators of transcription (STAT). *Eur J Neurosci* 2000; **12**: 1165–1176.
25. Liu RY, Snider WD. Different signaling pathways mediate regenerative versus developmental sensory axon growth. *J Neurosci* 2001; **21**: RC164.
26. Yamashita T, Sawamoto K, Suzuki S, Suzuki N, Adachi K, Kawase T *et al.* Blockade of interleukin-6 signaling aggravates ischemic cerebral damage in mice: possible involvement of Stat3 activation in the protection of neurons. *J Neurochem* 2005; **94**: 459–468.
27. Leibinger M, Muller A, Andreadaki A, Hauk TG, Kirsch M, Fischer D. Neuroprotective and axon growth-promoting effects following inflammatory stimulation on mature retinal ganglion cells in mice depend on ciliary neurotrophic factor and leukemia inhibitory factor. *J Neurosci* 2009; **29**: 14334–14341.
28. Komine-Kobayashi M, Zhang N, Liu M, Tanaka R, Hara H, Osaka A *et al.* Neuroprotective effect of recombinant human granulocyte colony-stimulating factor in transient focal ischemia of mice. *J Cereb Blood Flow Metab* 2006; **26**: 402–413.
29. Lin TN, Wang PY, Chi SI, Kuo JS. Differential regulation of ciliary neurotrophic factor (CNTF) and CNTF receptor alpha (CNTFR alpha) expression following focal cerebral ischemia. *Brain Res Mol Brain Res* 1998; **55**: 71–80.
30. Loddick SA, Turnbull AV, Rothwell NJ. Cerebral interleukin-6 is neuroprotective during permanent focal cerebral ischemia in the rat. *J Cereb Blood Flow Metab* 1998; **18**: 176–179.
31. Suzuki S, Tanaka K, Nogawa S, Nagata E, Ito D, Dembo T *et al.* Temporal profile and cellular localization of interleukin-6 protein after focal cerebral ischemia in rats. *J Cereb Blood Flow Metab* 1999; **19**: 1256–1262.
32. Herrmann O, Tarabin V, Suzuki S, Attigah N, Coserea I, Schneider A *et al.* Regulation of body temperature and neuroprotection by endogenous interleukin-6 in cerebral ischemia. *J Cereb Blood Flow Metab* 2003; **23**: 406–415.
33. MacLaren RE, Buch PK, Smith AJ, Balaggan KS, MacNeil A, Taylor JS *et al.* CNTF gene transfer protects ganglion cells in rat retinae undergoing focal injury and branch vessel occlusion. *Exp Eye Res* 2006; **83**: 1118–1127.
34. Dobrea GM, Unnerstall JR, Rao MS. The expression of CNTF message and immunoreactivity in the central and peripheral nervous system of the rat. *Brain Res Dev Brain Res* 1992; **66**: 209–219.
35. Friedman B, Scherer SS, Rudge JS, Helgren M, Morrisey D, McClain J *et al.* Regulation of ciliary neurotrophic factor expression in myelin-related Schwann cells *in vivo*. *Neuron* 1992; **9**: 295–305.

36. Rende M, Muir D, Ruoslahti E, Hagg T, Varon S, Manthorpe M. Immunolocalization of ciliary neuronotrophic factor in adult rat sciatic nerve. *Glia* 1992; **5**: 25–32.
37. Sendtner M, Stockli KA, Thoenen H. Synthesis and localization of ciliary neurotrophic factor in the sciatic nerve of the adult rat after lesion and during regeneration. *J Cell Biol* 1992; **118**: 139–148.
38. Sendtner M, Gotz R, Holtmann B, Thoenen H. Endogenous ciliary neurotrophic factor is a lesion factor for axotomized motoneurons in adult mice. *J Neurosci* 1997; **17**: 6999–7006.
39. Curtis R, Scherer SS, Somogyi R, Adryan KM, Ip NY, Zhu Y *et al.* Retrograde axonal transport of LIF is increased by peripheral nerve injury: correlation with increased LIF expression in distal nerve. *Neuron* 1994; **12**: 191–204.
40. Bourde O, Kiefer R, Toyka KV, Hartung HP. Quantification of interleukin-6 mRNA in wallerian degeneration by competitive reverse transcription polymerase chain reaction. *J Neuroimmunol* 1996; **69**: 135–140.
41. Marz P, Cheng JG, Gadient RA, Patterson PH, Stoyan T, Otten U *et al.* Sympathetic neurons can produce and respond to interleukin 6. *Proc Natl Acad Sci USA* 1998; **95**: 3251–3256.
42. Reichert F, Levitzky R, Rotshenker S. Interleukin 6 in intact and injured mouse peripheral nerves. *Eur J Neurosci* 1996; **8**: 530–535.
43. Hans VH, Kossmann T, Lenzlinger PM, Probstmeier R, Imhof HG, Trentz O *et al.* Experimental axonal injury triggers interleukin-6 mRNA, protein synthesis and release into cerebrospinal fluid. *J Cereb Blood Flow Metab* 1999; **19**: 184–194.
44. Raineteau O, Schwab ME. Plasticity of motor systems after incomplete spinal cord injury. *Nat Rev Neurosci* 2001; **2**: 263–273.
45. Bareyre FM, Kerschensteiner M, Raineteau O, Mettenleiter TC, Weinmann O, Schwab ME. The injured spinal cord spontaneously forms a new intraspinal circuit in adult rats. *Nat Neurosci* 2004; **7**: 269–277.
46. Yamagishi S, Fujitani M, Hata K, Kitajo K, Mimura F, Abe H *et al.* Wallerian degeneration involves Rho/Rho-kinase signaling. *J Biol Chem* 2005; **280**: 20384–20388.
47. Tanaka T, Ueno M, Yamashita T. Engulfment of axon debris by microglia requires p38 MAPK activity. *J Biol Chem* 2009; **284**: 21626–21636.

特集「シャルコー・マリー・トゥース病の診断と治療」

シャルコー・マリー・トゥース病の外科的治療*

渡邉　耕太，山下　敏彦

要旨　CMT病では足に対する手術が多い。足部の変形は内反足、尖足、凹足、鉤爪趾変形などが組み合わされ、下垂足も合併する。軟部組織に対する手術としては、足底解離術、筋腱移行術、アキレス腱延長術などがある。骨に対する手術は各種の骨切術や関節固定術が行われている。手の変形は鉤爪手が特徴的である。腱移行術、関節固定術、軟部組織解離術、神経除圧術などが行われる。股関節では臼蓋形成不全を合併することがあり、手術療法としては骨切術が行われる。脊椎では側弯変形がみられることがあり、後弯変形も伴うことがある。治療は、一般に特発性側弯症に対するのと同様な方法で行われる。手術により疼痛や機能を改善する効果が期待できる。

Key Words : シャルコー・マリー・トゥース病，手術，手／足変形，凹足，末梢神経疾患

Peripheral Nerve 2011; 22(1): 22–30

シャルコー・マリー・トゥース病における手術適応について

シャルコー・マリー・トゥース病（以下CMT）では、両側下肢遠位筋から始まる脱力と筋萎縮が徐々に進行することにより足の変形を生じる。そのため、手術治療は足に行われることが多くなる。CMTの筋力低下は足内在筋から始まり、短腓骨筋、前脛骨筋、腓腹筋の順に障害されるといわれている。障害された筋とその拮抗筋との筋緊張のバランスが崩れることにより、特徴的な足変形をきたす。内反足、尖足、凹足、鉤爪趾変形などの変形が組み合わされ、足関節背屈筋麻痺による下垂足も合併する。拘縮予防や筋力訓練などのリハビリテーションや装具療法によっても歩行障害の改善が小さい場合や、変形に伴う足部の疼痛や皮膚潰瘍の問題が生じる場合には手術治療が必要になる。

足に遅れて手にも麻痺が生じるので、手に対する手術治療も必要になることがある。また、股関節の臼蓋形成不全や脊柱変形の合併も報告されており、手術治療が行われている。

CMTに対する主な手術療法

足の手術

前述のようにCMTの足部変形は、内反足、尖足、凹足、鉤爪趾変形などの変形が組み合わされ、足関節背屈筋麻痺による下垂足も合併する。それぞれの変形の程度はさまざまであるので、各症例に応じた手術計画を立てる必要がある。最も一般的な変形は内反凹足である。足内在筋の萎縮と拘縮により足の縦アーチが挙上する。また、後脛骨筋と長腓骨筋の筋力は短腓骨筋や前脛骨筋の麻痺に比べて残存するので、この筋力不均衡により第1中足骨の底屈や足の内反変形が助長されることとなる[1]。

* Surgical treatment for patients with Charcot-Marie-Tooth disease

Kota WATANABE and Toshihiko YAMASHITA：札幌医科大学医学部整形外科［〒060-8543 札幌市中央区南1条西16丁目］；Department of Orthopaedic Surgery, Sapporo Medical University School of Medicine, Sapporo

1．内反凹足

若年時に腱移行を含む軟部組織手術を行うことにより、将来的な三関節固定術の時期を遅らせるか不要とすることが可能となる。

① 足底解離術：踵骨内側に皮切をおき、足底筋膜を踵骨から切離する（図1）。

術後後療法；この手術が単独で行われることはまれである。単独で行った場合には3週間のギプス固定と免荷を行う。さらに3週間歩行用ギプスを装着する。

② 長腓骨筋腱の短腓骨筋腱への移行術：この腱移行により長腓骨筋の第1中足骨を底屈させる作用を減じ、かつ足外反力を増加させる。

③ 後脛骨筋腱背側移行術：足関節背屈筋力の低下した下垂足に有効である。後脛骨筋腱を骨付着部で切離し、開窓した骨間膜を通して足背側へ引き出し、足背側の骨へ腱固定する（図2）。足関節背屈力を増加するとともに、足内反変形を生じさせる力を減じることができる。

術後後療法；腱移行術後は約6週間のギプス固定を行う。リハビリテーションでは筋力訓練とともに、移行した筋が歩行周期に合わせてタイミング良く収縮するように再教育することも重要となる。

軟部組織手術でも矯正しえない変形には、骨に対する手術が必要である。

④ 中足骨骨切術：中足骨を近位部で骨切し、背屈固定することで凹足変形を矯正する（図3）。変形の強い症例では複数の中足骨に対する矯正骨切術が必要になる。

⑤ 踵骨骨切術：踵骨外側から踵骨に至り骨切した後、踵骨後方部を外側や上方に移動したり、外側を底部とする楔状に骨を切除するなどにより内反凹足を矯正する（図4）。

⑥ 中足部骨切術：中足部を背側に底部を持つ楔状に骨切除をする（Cole）、V字に骨切する（Japas）、足根中足関節を切除する（Jahss）などの骨切法がある。変形を矯正して骨切部を固定する（図5）。

術後後療法；骨切術後はギプス固定を行う。術後数週は免荷が必要である。踵骨骨切術では5週後から歩行用ギプスを装着し歩行練習を行う。中足骨近位骨切術や中足部骨切術では6週間のギプスによる固定と、それに引き続き歩行用ギプスを装着する（骨癒合が得られるまで）。

⑦ 三関節固定術：変形が高度で軟部組織手術や骨切術によって十分な矯正が得られない場合に適応となる術式である。種々の方法が報告されている（図6）。変形が高度の場合には大きな骨切除を要する場合がある。

術後後療法；ギプス固定を行う。6週間免荷し、レントゲンで骨癒合を確認しつつ歩行用ギプスとする。10週程度で骨癒合が確認できたら、ギプス除去となる。

三関節固定術後には長期経過後に隣接関節に変性変化が生じて痛みの原因になることがある。三関節固定術を平均年齢15歳の症例に行った長期経過（平均21年）報告では、約半数で疼痛や変形再発のため成績不良であったとの報告がある。そのため若年者に対

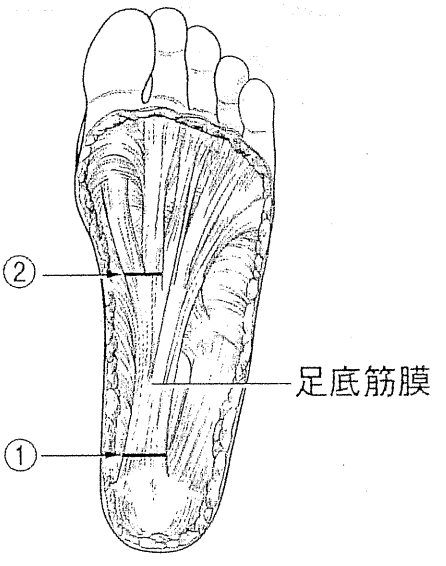

図1　足底筋膜切離術
筋膜切離部は図の①だけでなく、②にも追加されることがある。

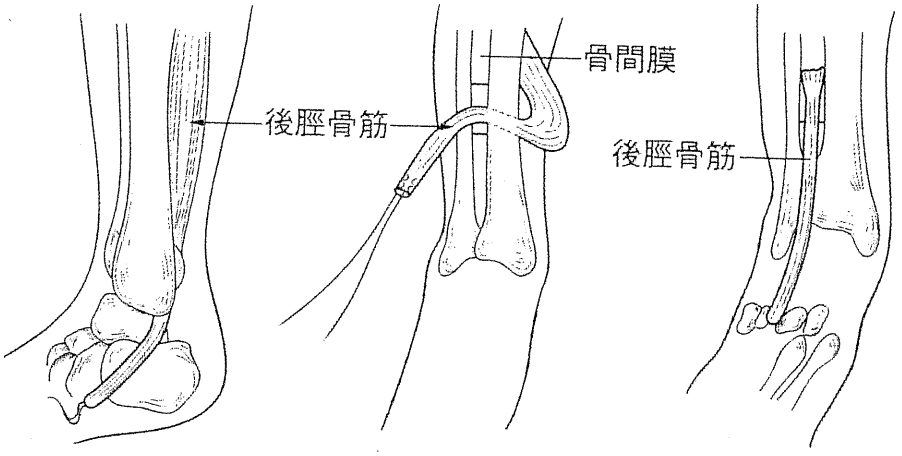

図2　後脛骨筋腱背側移行術
後脛骨筋腱を骨付着部で切離し、開窓した骨間膜を通して足背側へ引き出し、足背側の骨へ腱固定する。

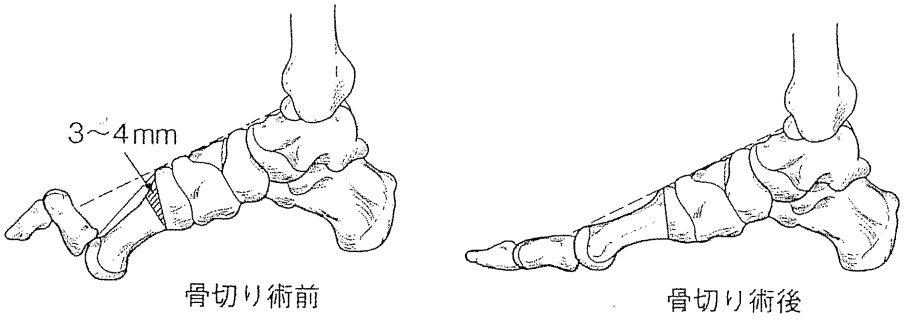

図3　中足骨骨切術
中足骨の近位部で骨切を行い、底屈した中足骨を矯正して骨の固定を行う。

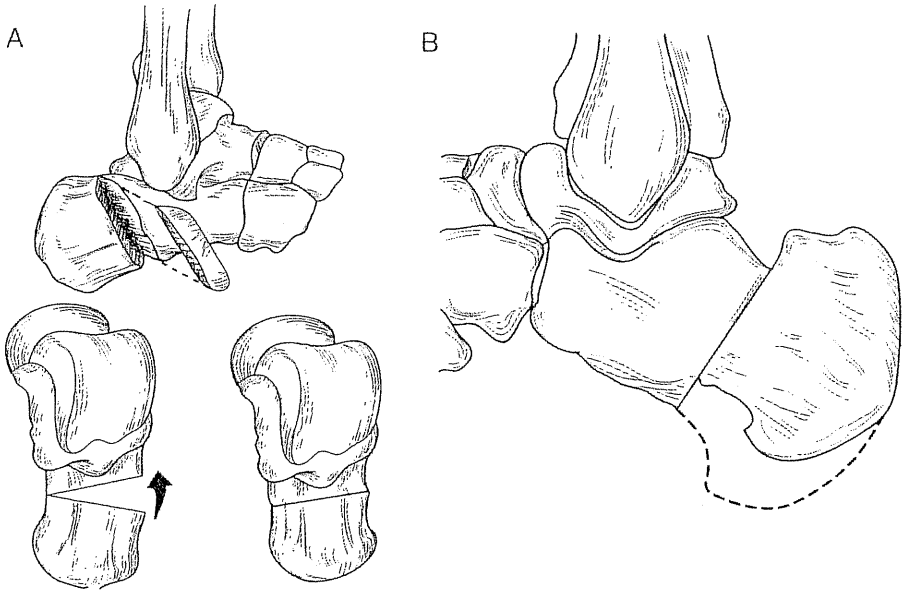

図4　踵骨骨切術
A：踵骨外側を底部とする楔状に骨を切除し固定する（Dwyer法）。
B：踵骨を骨切した後に、後方部分を上方に移動させ固定する。

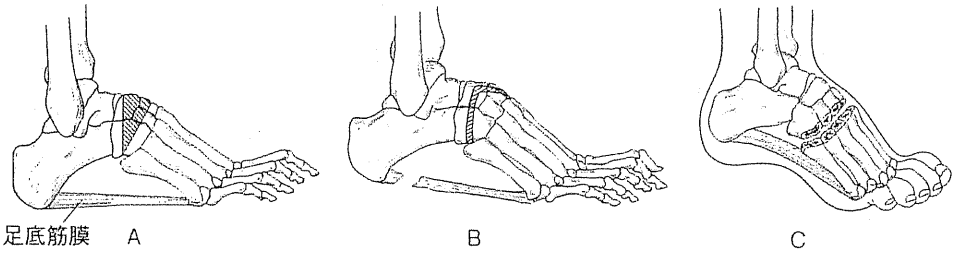

図5　中足部骨切術
A：Cole法，B：Japas法，C：Jahss法

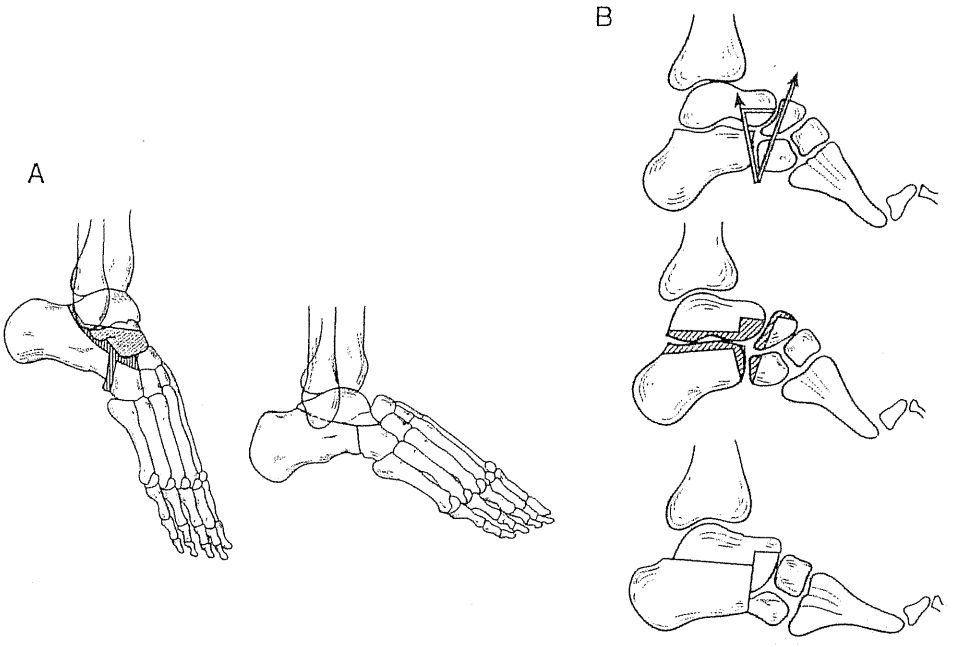

図6　三関節固定術
斜線部を切除して固定する。
A：Lambrinudi法，B：Stiffert法

する三関節固定術は、以前に行った手術の再発例や、変形が高度で可動性のない症例に限るべきであると考えられている[2)]。

2．鉤爪趾変形

低下した足関節背屈力を補うために足趾伸筋が強く働くことと、中足骨の底屈変形のために、足趾のMTP関節が背屈しPIP関節とDIP関節が屈曲するという変形が生じる。この変形をきたすと、荷重時に中足骨底側への圧が高まることで同部位に胼胝や場合によっては潰瘍を形成する。

手術治療として、母趾のIP関節固定と長母趾伸筋腱を第1中足骨頭へ移行する術式（Jones法）がある。この腱移行により中足骨を背屈させる効果が期待できる。長趾伸筋腱を楔状骨へ移行する方法（Hibbs法）では、足趾の変形矯正と足関節背屈力増加の効果が期待できる（図7）。

術後後療法；長母趾伸筋腱移行術（Jones法）後は歩行用ギプスを4週から6週装着する。

3．尖足

アキレス腱延長術：Sliding lengthening法はアキレス腱を3か所で半切してから、他動的に足関節を背屈強制し延長する方法である

(図8)。Z延長術を行う場合には、CMTでは内反足も伴うため、腱の踵骨付着部は外側を残すようにしてアキレス腱による内反力を減じるようにする。

術後後療法；術後4週から6週のギプス固定を行う。

4．下垂足

前述の後脛骨筋腱背側移行術が適応となる。年齢が高く変形性足関節症が高度で疼痛をきたしている場合や手術後の再発例には、足関節固定術が必要になる。

CMTによる足部変形に対する手術治療では、低年齢時の変形に可動性がある状態に対して軟部組織手術を行うことで、より侵襲の大きい手術を行う時期を遅らせることが可能である。また、関節外の骨切術を併用することで、関節機能を温存しつつより有効な変形矯正が行える。手術後の再発例や可動性のない高度の変形を呈している場合には、三関節固定術により変形矯正や歩行能の改善が得られる。

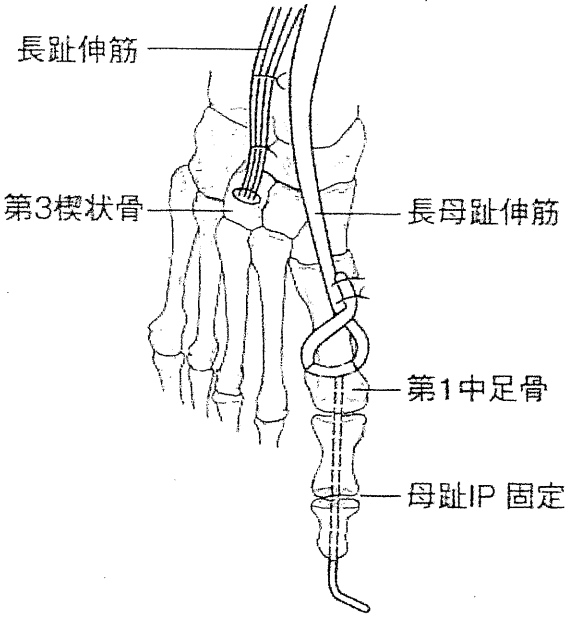

図7　鉤爪変形に対する手術
Jones法では長母趾伸筋腱（EHL）を切離し、中足骨頭に作製した骨孔を通して固定する。
Hibbs法では長趾伸筋腱（EDL）を切離し、第3楔状骨に固定する。

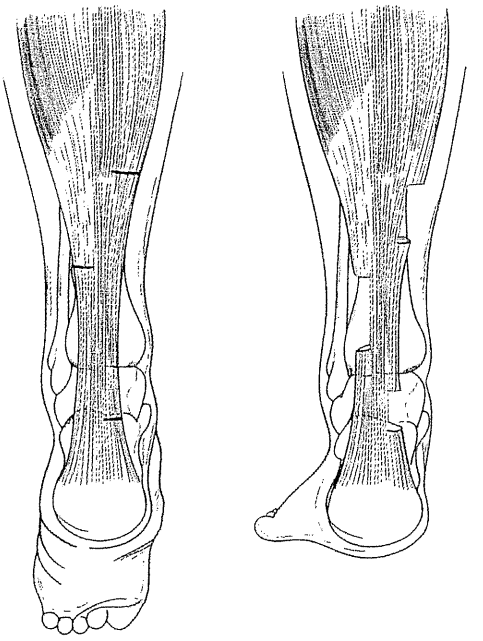

図8　アキレス腱延長術
Sliding lengthening法では、3か所でアキレス腱を横切し、足関節を背屈強制することでアキレス腱を延長する。この方法では腱縫合は不要である。

CMTの手術治療において気をつけなくてはならないことの一つとして、麻痺は進行性のため術直後の変形矯正が良好であっても将来的に三関節固定術や足関節固定術などの再手術が必要となる可能性のあることが挙げられる。

手の手術

上肢の障害はCMTの1／2から2／3に出現するといわれている。まず手内在筋の筋力低下が出現する。外在筋の麻痺はそれに遅れて出現する。手の変形は鉤爪手が特徴的である。さらに病状が進行すると尺骨神経に加えて正中神経の麻痺も生じ、鉤爪手変形はより顕著となる。それらに比べて橈骨神経麻痺の発生は少ないといえる。

筋力低下とともにつまみ動作や母指対立運動などの機能が障害される。また関節症や腱鞘炎による疼痛、関節拘縮なども生じる。感覚障害による症状もきたす。